Stable modal identification for civil structures based on a stochastic subspace algorithm with appropriate selection of time lag parameter

Wen-Hwa Wu[*1], Sheng-Wei Wang[2a], Chien-Chou Chen[1b] and Gwolong Lai[1c]

[1]*Department of Construction Engineering, National Yunlin University of Science and Technology, 123 University Road, Douliu, Yunlin 640, Taiwan*
[2]*Intelligent Electronic Systems Division, National Chip Implementation Center, National Applied Research Laboratories, Hsinchu City 300, Taiwan*

Abstract.   Based on the alternative stabilization diagram by varying the time lag parameter in the stochastic subspace identification analysis, this study aims to investigate the measurements from several cases of civil structures for extending the applicability of a recently noticed criterion to ensure stable identification results. Such a criterion demands the time lag parameter to be no less than a critical threshold determined by the ratio of the sampling rate to the fundamental system frequency and is firstly validated for its applications with single measurements from stay cables, bridge decks, and buildings. As for multiple measurements, it is found that the predicted threshold works well for the cases of stay cables and buildings, but makes an evident overestimation for the case of bridge decks. This discrepancy is further explained by the fact that the deck vibrations are induced by multiple excitations independently coming from the passing traffic. The cable vibration signals covering the sensor locations close to both the deck and pylon ends of a cable-stayed bridge provide convincing evidences to testify this important discovery.

Keywords: alternative stabilization diagram; stochastic subspace identification; civil structure; time lag parameter; multiple excitations

1. Introduction

Mainly because of the advantages in easy operation and low cost, the modal identification and health monitoring of civil engineering structures have been more popularly conducted in recent years with ambient vibration measurements. The operational modal analysis simply using the output signals is indispensable in such applications to effectively obtain the modal frequencies, damping ratios, and mode shape vectors. Attributing to the research progress over the past few decades, a number of output-only modal identification methods are currently available, either via

---

∗Corresponding author, Professor, E-mail: wuwh@yuntech.edu.tw

[a] Postdoctoral Research Associate, Email: shengweiwang0426@gmail.com
[b] Professor, Email: ccchen@yuntech.edu.tw
[c] Associate Professor, Email: laig@yuntech.edu.tw

the frequency domain or the time domain analysis. Among all these output-only identification techniques, stochastic subspace identification (SSI) has soon developed into a benchmark method with its sound mathematical basis and wide applicability. Van Overschee and De Moor first proposed the commonly adopted formulation of SSI (Van Overschee and De Moor 1991) and subsequently established the corresponding algorithm for modal parameter identification (Van Overschee and De Moor 1996, Van Overschee and De Moor 1993). Several essential techniques in linear algebra such as QR (or LQ) decomposition, singular value decomposition (SVD), and oblique projection were employed in their theoretical derivation and solution algorithm. This series of methods are usually referred as the data-driven SSI due to the direct processing of the output matrix from measurements. Other than the data-driven SSI, the covariance-driven SSI was later proposed by Peeters (2000) to conduct SSI with the covariance matrix of output measurements. The covariance-driven SSI holds the benefits in simpler mathematical derivation and computational efficiency. Certain studies (Mevel *et al.* 2003, Reynders *et al.* 2008) also reported that the results obtained from the covariance-driven SSI algorithms are typically more stable.

The applications of SSI techniques in civil engineering structures such as bridges and buildings have been rapidly grown in the past decade, especially focusing on the fields of system identification (Reynders and De Roeck 2008, Magalhaes *et al.* 2010, Sampaio and Chan 2015), structural health monitoring (Deraemaeker *et al.* 2008), and damage detection (Yan and Golinval 2006, Kompalka *et al.* 2007). Nevertheless, a few difficulties are still encountered in these practical cases. One of the most critical problems comes from the fact that the actual process and measurement noises of a civil structure are generally dissimilar to the zero-mean, white-noise, and stationary assumptions adopted in the derivation of SSI method. Various degrees of error are consequently induced in modal identification with different selected values of the time lag parameter and the system order parameter, both necessary to be prescribed in conducting the SSI analysis. The stabilization diagram is normally utilized to systematically assess this problem by displaying the gradually increased system order along the ordinate and the corresponding modal frequencies along the abscissa under an assigned value of the time lag parameter. With this presentation, it is expected that the actual physical modes can be evidently distinguished by gathering at separated narrow neighborhoods of stable frequency values. On the other hand, the frequency values of spurious mathematical modes usually scatter around. This concept of employing the stabilization diagram was also explored in recent studies (Cara *et al.* 2012, Loh *et al.* 2012, Cara *et al.* 2013) to handle the cases with close modes or other complicated situations. To reach the ultimate goal of an automated SSI analysis (Magalhaes *et al.* 2009, Reynders *et al.* 2012, Ubertini *et al.* 2013), proper discrimination criteria based on theories like clustering analysis (Scionti and Lanslots 2005, Carden and Brownjohn 2008, Bakir 2011) need to be further applied for the systematic extraction of effective physical modes from the stabilization diagram.

As previously described, the conventional stabilization diagram illustrates the frequencies calculated at a fixed value of the time lag parameter. For the applications in civil structures often subjected to narrowly banded excitations, however, the selection of time lag parameter may has a strong influence on the determined modal parameters (Magalhaes *et al.* 2009). The great uncertainty of actual excitations in these cases makes it particularly difficult to obtain a clear criterion for choosing the time lag parameter. Instead, certain heuristic rules were adopted in the literature such as the one that the shift of measurements manipulated by the time lag parameter should cover a sufficiently large number of cycles of the lowest frequency (Magalhaes *et al.* 2009, Ubertini *et al.* 2013). Until very recently, a work by the authors (Wu *et al.* 2014, Wu *et al.* 2016a) revealed that the lower limit for setting the time lag parameter can be decided with the ratio of the

fundamental period of a stay cable to the sampling time increment for a valid modal identification using the conventional stabilization diagram. Inspired by this important criterion, a new methodology based on the covariance-driven SSI was established by proposing an alternative stabilization diagram to exhibit the results with varying values of the time lag parameter for more conveniently distinguishing stable modal parameters of cable. A hierarchical sifting process with three stages was also developed to automatically extract reliable modal parameters from the alternative stabilization diagram. Equipped with this improved SSI algorithm, a related study (Wu *et al.* 2016b) further investigated a benchmark problem for the mode identifiability of a cable-stayed bridge by analyzing several sets of known and blind bridge deck measurements.

Exploiting the advantages of such an alternative stabilization diagram, this study aims to more systematically examine the newly discovered criterion for choosing the time lag parameter in the application of stay cables and hopes to further generalize its applicability to the other cases of civil structures. Aside from inspecting the signals from stay cables in depth for more comprehensive understanding, the ambient vibration measurements of bridge decks and buildings are explored in the current work as well. Moreover, the effect of independent excitations on the appropriate selection of time lag parameter is also discussed.

2. Stochastic subspace identification and alternative stabilization diagraming

The procedures of the covariance-driven SSI are briefly reviewed in this section first, followed by introducing the concepts of alternative stabilization diagram.

2.1 Covariance-driven stochastic subspace identification

The derivation of SSI methods typically starts from the state space description of a linear dynamic system with n degrees of freedom (DOF). If output measurements are conducted to obtain the $l \times 1$ output vector $y(k)$ at the time instant $k\Delta t$ and Δt symbolizes the sampling time increment, the output vectors measured at N consecutive time instants can be systematically organized into a Hankel matrix with the selection of a time lag parameter i

$$\mathbf{Y}_{0|2i-1} = \frac{1}{\sqrt{j}} \begin{bmatrix} \mathbf{y}(0) & \mathbf{y}(1) & \cdots & \mathbf{y}(j-1) \\ \mathbf{y}(1) & \mathbf{y}(2) & \cdots & \mathbf{y}(j) \\ \vdots & \vdots & \ddots & \vdots \\ \mathbf{y}(i-1) & \mathbf{y}(i) & \cdots & \mathbf{y}(i+j-2) \\ \mathbf{y}(i) & \mathbf{y}(i+1) & \cdots & \mathbf{y}(i+j-1) \\ \mathbf{y}(i+1) & \mathbf{y}(i+2) & \cdots & \mathbf{y}(i+j) \\ \vdots & \vdots & \ddots & \vdots \\ \mathbf{y}(2i-1) & \mathbf{y}(2i) & \cdots & \mathbf{y}(2i+j-2) \end{bmatrix}_{2il \times j} = \begin{bmatrix} \mathbf{Y}_{0|i-1} \\ \mathbf{Y}_{i|2i-1} \end{bmatrix} = \begin{bmatrix} \mathbf{Y}_p \\ \mathbf{Y}_f \end{bmatrix} \tag{1}$$

where $\mathbf{Y}_p$ and $\mathbf{Y}_f$ are both $il \times j$ with $j = N - 2i + 1$. Post-multiplication of $\mathbf{Y}_f$ by $\mathbf{Y}_p^T$ leads to the approximation of the so-called Toeplitz matrix **T**. Singular value decomposition can then be conducted on $\mathbf{Y}_f \mathbf{Y}_p^T$ to obtain

$$\mathbf{Y}_f\mathbf{Y}_p^{\mathrm{T}} = \mathbf{USV}^{\mathrm{T}} = \left[(\mathbf{U}_1)_{il\times 2n} \quad (\mathbf{U}_2)_{il\times n_1}\right]\begin{bmatrix}(\mathbf{S}_1)_{2n\times 2n} & \mathbf{0}_{2n\times n_1} \\ \mathbf{0}_{n_1\times 2n} & (\mathbf{S}_2)_{n_1\times n_1}\approx\mathbf{0}_{n_1\times n_1}\end{bmatrix}\begin{bmatrix}(\mathbf{V}_1^{\mathrm{T}})_{2n\times il} \\ (\mathbf{V}_2^{\mathrm{T}})_{n_1\times il}\end{bmatrix}\approx\mathbf{U}_1\mathbf{S}_1\mathbf{V}_1^{\mathrm{T}} \tag{2}$$

where $n_1 = il - 2n$, $\mathbf{U}$ and $\mathbf{V}$ are orthogonal matrices, and $\mathbf{S}$ is a quasi-diagonal matrix with positive diagonal elements arranged in a decreasing order. By further taking

$$\mathbf{O}_i = \mathbf{U}_1\mathbf{S}_1^{1/2} \quad\text{and}\quad \mathbf{\Gamma}_i = \mathbf{S}_1^{1/2}\mathbf{V}_1^{\mathrm{T}} \tag{3}$$

it has been shown (Peeters 2000) that the discretized system matrix $\mathbf{A}$ in the state space can be determined by

$$\mathbf{A} = \mathbf{O}_i^{\oplus}\big(1:l(i-1),:\big)\mathbf{O}_i\big(l+1:li,:\big) \tag{4}$$

where the symbol $\oplus$ denotes the pseudo inverse operation. With the discretized system matrix $\mathbf{A}$, its eigenvalues $\tilde{\lambda}_k$'s are solved and then used to calculate the related eigenvalues λ_k's of the continuous system matrix $\mathbf{A}_c$ that incorporates the mass, damping, and stiffness matrices in the state space. Based on the theory of linear systems, the modal frequencies ω_k's and damping ratios ξ_k's of the system can be directly calculated from λ_k's which theoretically appear in complex-conjugate pairs. Besides, the eigenvectors of $\mathbf{A}_c$ are identical to as those of $\mathbf{A}$ from the matrix theory and can be used to obtain the mode shape vectors at the output measurement locations $\boldsymbol{\varphi}_k$'s.

From the above review, it is obvious that the time lag parameter i in Eq. (1) and the system order parameter n in Eq. (2) have to be prescribed in conducting the SSI analysis. Theoretically, the time lag parameter specifies the construction of a Hankel matrix from the measured signals and the subsequent modal parameters identified in the SSI analysis should be insensitive to its value if the excitation is close to the white-noise assumption. It is not this case, however, when the excitation is narrowly banded. As for the system order parameter n, it indicates the selection of the largest $2n$ sigular values in Eq. (2) to compose the two matrices in Eq. (3) and consequently decides the size of the discretized system matrix $\mathbf{A}$ to finally provide n sets of modal parameters. A value of n sufficiently larger than the number of physical modes within the interested frequency range is usually chosen to assure the incorporation of more contributing modes. The use of high model orders may also result in the inclusion of spurious numerical modes, but is necessary for identifying weakly excited modes and can be helpful to model the noise always existed in measured data (Magalhaes *et al*. 2009, Ubertini *et al*. 2013).

2.2 Alternative stabilization diagram

The determination of modal parameters with the SSI analysis conventionally requires constructing the stabilization diagram to observe the stability of the identified results with the increasing value of n under a designated value of i. Nevertheless, the performance of stabilization diagrams for the applications in civil structures can be significantly affected by the selection of time lag parameter. An effort was made in a recent research by the authors (Wu *et al*. 2014, Wu *et al*. 2016a) to resolve this discrepancy in identifying the modal parameters of a stay cable. Considering the fact that all the modal frequencies of a stay cable are with values approximately in

integer multiples of its fundamental frequency f_1, it was first pointed out that the ambient vibration signal of cable would be nearly a periodic function with a quasi-period close to the period $T_1 = 1/f_1$ of the first cable mode. Therefore, all the possible independent patterns of the covariance for the output vector would be uniformly incorporated in $\mathbf{Y}_f \mathbf{Y}_p^{\mathrm{T}}$ if

$$i \geq i_c = \frac{T_1}{\Delta t} = \frac{s}{f_1}$$

(5)

where $s = 1/\Delta t$ represents the sampling rate of measurement and i_c means the critical threshold for the time lag parameter to ensure stable identification results. Compared with the heuristic rule that the time lag parameter should be taken to cover a few cycles of the lowest frequency (Magalhaes *et al.* 2009, Ubertini *et al.* 2013), the criterion of Eq. (5) is certainly more specific and economical for computation. The SSI analysis was performed for the ambient vibration measurements taken on three stay cables of Chi-Lu Bridge to verify this criterion. Even for the measurements on the other structures with irregularly distributed modal frequencies, Eq. (5) is also expected to be practically applicable because the unbiased distribution of all the possible independent patterns of $\mathbf{H}_m$ may still be roughly attained with this condition.

Inspired by the criterion of Eq. (5), that recent work (Wu *et al.* 2014, Wu *et al.* 2016a) further proposed an alternative stabilization diagram which exhibits the gradually increased time lag parameter *i* along the ordinate and the corresponding modal frequencies along the abscissa under an assigned value of the system order *n*. By first examining the Fourier amplitude spectra (FAS) of cable signals, it was suggested to choose the system parameter *n* that is approximately twice of the observable peaks (Ubertini *et al.* 2013) and determine the fundamental period of cable for setting the lower limit $i_{\min} = i_c$ with Eq. (5). In addition, the upper limit of time lag parameter $i_{\max}$ is decided by the need in the subsequent processes to extract reliable modal parameters. The alternative stabilization diagram has also been validated to hold the advantage in less interference from the superfluous modes for the cases of stay cables (Wu *et al.* 2016a).

3. Investigated structures and measurements

For extensively evaluating the applicability of the critical threshold for the time lag parameter shown in Eq. (5), two cable-stayed bridges and a reinforced concrete building are selected in this research for investigation and will be introduced in the subsequent subsections. The high resolution velocimeters VSE-15D made by Tokyo Sokushin were employed to conduct the ambient vibration measurements on these structures. A portable ambient vibration monitoring system SPC-51 with a maximum sampling frequency of 1000 Hz, also from Tokyo Sokushin, was connected with the VSE-15D sensors to collect the signals. In all the measurements, the duration was set at 300 sec with a sampling rate of $s = 200$ Hz.

3.1 Chi-Lu Bridge and measurements of its stay cables and deck

As illustrated in Fig. 1, Chi-Lu Bridge locates in central Taiwan to connect the two towns Chi-Chi and Lu-Ku. It is a single-pylon symmetric cable-stayed bridge built by pre-stressed
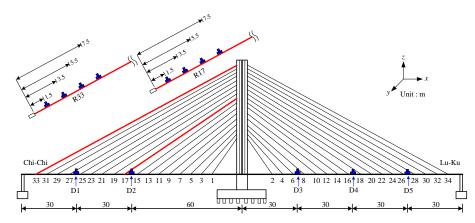
Fig. 1 Chi-Lu Bridge and its sensor locations

concrete box girders, comprising two 120 m main spans. The single-plane cable system, as shown in Fig. 1, consists of 17 pairs of stay cables on each side of the pylon and is arranged in the semi-fan shape The ambient vibration measurements were first conducted on two cables of Chi-Lu Bridge: R33 and R17, representing the longest and medium cable, respectively. Cable R33 is 126.4 m long with an inclination angle of 26° and Cable R17 is 76.4 m long with an inclination angle of 31°. Moreover, the ambient vibration signals at different locations of the bridge deck are also taken in this study for further analysis.

To estimate the mode shape ratios of cable required in a recently developed methodology by the authors for the determination of its tension (Chen *et al.* 2013), four velocimeters were installed on each cable to record the synchronized vibration signals in the in-plane direction perpendicular to the axial orientation of cable. Considering the convenience in practical applications, all these sensor locations were selected to be close to the bridge deck. Their distances to the front end of the bottom rubber constraint are also indicated in Fig. 1 to be 1.5 m, 3.5 m, 5.5 m, and 7.5 m, respectively. As for the measurements on the bridge deck, five velocimeters were deployed along the central line of deck to simultaneously collect the velocity responses in the gravity direction. Denoted by D1 to D5, these five sensors were arranged at distances of 30 m, 60 m, 150 m, 180 m, and 210 m from the Chi-Chi end.

3.2 Shin-Dong Bridge and measurements on its stay cables

As depicted in Fig. 2, Shin-Dong Bridge is a three-span (75 m+175.6 m+75 m) cable-stayed bridge connecting Miau-Li and Kong-Kuang located in northern Taiwan. It is a double-pylon symmetric bridge made by steel box girders and its cable system consists of 34 stay cables, 9 on the outer side and 8 on the inner side of each pylon. Installation of sensors close to the pylon end of a stay cable is usually difficult in practical implementation. It is fortunate that this research group had an opportunity in 2014 to conduct a measurement project on Shin-Dong Bridge for evaluating a novel method used in accurately estimating the cable force (Wu *et al.* 2012, Chen *et al.* 2016). The ambient vibration measurements were taken on Cables C16 and C13, both on the outer side of the pylon close to the Miau-Li end. Cable C16 is 86.8 m long with an inclination angle of 31° and Cable C13 is 63.1 m long with an inclination angle of 36°. A total of four sensors

were adopted to record the synchronized vibration signals of each cable in the in-plane vertical direction normal to cable. Three velocimeters were mounted close to the deck end. On the other hand, the forth velocimeter near the pylon end needs to be installed with the help of a hired crane. For Cable C16, the distances of sensors to the front end of the bottom rubber constraint are 4.0 m, 5.5 m, 7.0 m, and 72.6 m, respectively. For Cable C13, the corresponding distances are 3.5 m, 5.0 m, 6.3 m, and 52.0 m, respectively.
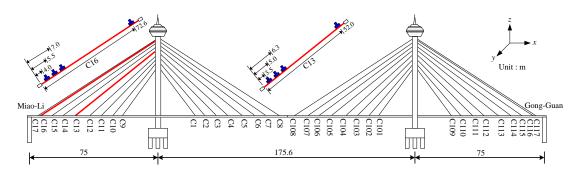

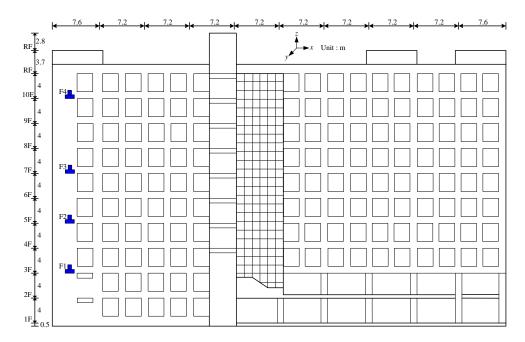Fig. 2 Shin-Dong Bridge and its sensor locations

Fig. 3 Electronic and Environmental Engineering Building and its sensor locations

3.3 Electronic and Environmental Engineering Building at YUNTECH and measurements on its floors

Electronic and Environmental Engineering (EEE) Building sits on the campus of National Yunlin University of Science and Technology (YUNTECH) located in central Taiwan. As plotted in Fig. 3, this is a 10-story reinforced concrete building with a height of 47 m, a length of 72.8 m, and a width of 24.6 m. It is partitioned into classrooms and offices by brick walls. Other than an elevator and a stairway situated in the central portion, the other stairway is also positioned on one side. One velocimeter was mounted on each floor of 3F, 5F, 7F, and 10F, respectively, to record the synchronized vibration signals in the short (*y*) direction of building. Signified from F1 to F4 starting with the lower floor, all the sensors were installed near the side stairway which is seldom used by pedestrians for the convenience in conducting the ambient vibration measurements during working hours.

4. Appropriate choice of time Lag parameter

In addition to more effectively reduce the interference from the deceptive modes in SSI analysis, the alternative stabilization diagram recently proposed (Wu *et al.* 2014, Wu *et al.* 2016a) also provides an excellent tool to investigate the critical threshold for the time lag parameter. Even though the formula of Eq. (5) was found to be adequately accurate in the case of cable measurements (Wu *et al.* 2016a) to ensure stable modal frequencies, it seems to overestimate the lower limit for an appropriate choice of time lag parameter in the case of bridge deck measurements (Wu *et al.* 2016b). For conveniently clarifying the applicability of Eq. (5) in various types of structures, the current study starts in this section by examining the alternative stabilization diagrams for the cases simply with a single measurement. The same inspection on similar cases with multiple measurements will be followed for further discussions.

4.1 Single measurement

In this subsection, a single measurement either from the stay cable of Chi-Lu Bridge, the deck of Chi-Lu Bridge, and the floor of EEE Building is considered for performing the SSI analysis. It is apparent from Eq. (2) that

$$il - 2n = n_1 \geq 0 \qquad \text{or} \qquad i \geq 2n/l = i_0 \tag{6}$$

In other words, the lowest possible value of the time lag parameter i_0 is controlled by the choice of the system order parameter *n*. For the cases of a single measurement ($l = 1$), $i_0 = 2n$. To clearly observe the varying trend of identified modal frequencies, the lower limit of time lag parameter is consistently set at $i_{\min} = i_0$ in the subsequent alternative stabilization diagrams.

4.1.1 Cable measurements of Chi-Lu Bridge

Taking the ambient vibration measurement at 7.5 m from the front end of the bottom rubber constraint for Cable R33 as the first example, the system order is fixed at $n = 20$ because there are around 11 peaks observable in the interested frequency range from 0 to 10 Hz of the FAS for this measurement. The SSI analysis is then performed with the time lag parameter increasing from $i_{\min} = i_0 = 40$ to $i_{\max} = 320$ for establishing the alternative stabilization diagram shown in Fig.

4(a) where the identified frequencies values are symbolized by black cross signs together with the corresponding FAS displayed in the background. Since the fundamental frequency of Cable R33 is $f_1 \approx 0.9\,\text{Hz}$, the critical threshold can be determined to be $i_c = 200/0.9 \approx 220$ according to Eq. (5) and is also illustrated in Fig. 4(a) with a horizontal dashed line in red. Fig. 4(a) obviously confirms that all the identified cable frequencies are stable until the value of time lag parameter gets close to the criterion of $i \geq i_c = 220$. Moreover, the alternative stabilization diagram corresponding to the measurement at 7.5 m from the bottom rubber constraint for Cable R17 is further presented in Fig. 4(b). In this case, the system order parameter is also set as $n = 20$ based on the observation of approximately 8 peaks in the targeted frequency range from 0 to 15 Hz of the FAS. With the fundamental frequency of $f_1 \approx 1.63\,\text{Hz}$ for Cable R17, its critical threshold $i_c = 200/1.63 \approx 120$ can then be obtained and the SSI analysis is conducted from $i_{\min} = i_0 = 40$ to $i_{\max} = 220$ for constructing the alternative stabilization diagram. Without any surprise, the frequency associated with each cable mode reaches its stable values in Fig. 4(b) when the level of $i = i_c = 120$ is reached. To more systematically validate the criterion of Eq. (5), two artificial manipulations are imposed on the original single measurements of Cables R33 and R17 for additional investigations. First, the contribution of the first cable mode in each measurement is significantly reduced in an interval of 2/3 Hz symmetrically enclosing that peak in the frequency domain. More specifically, the Fourier amplitude in this interval is multiplied by a weighting function linearly decreased from 100% at the boundary to 2% at the central peak frequency.

The inverse Fourier transform is then taken to reconstruct the modified signal in the time domain, basically removing the contribution from the first cable mode. The alternative stabilization diagrams for the modified single measurements of Cables R33 and R17 with a suppression of the first mode are plotted in Fig. 5. Other than the disappearance of the first cable mode as expected, it is apparent from Fig. 5 that all the other cable frequencies are consistently stable until similar critical values of time lag parameter ($i_c = 220$ for Cable R33 and $i_c = 120$ for Cable R17) are reached. Again, this phenomenon can be explained by the fact that the cable frequencies are generally with values of an arithmetic sequence. Even if the contribution of the first mode is removed, the least common multiple for the periods of the rest modes is still T_1. Consequently, the modified signal would remain to be nearly a periodic function with a quasi-period close to T_1 and follows the same criterion for the time lag parameter as that for the original measurement. A subsidiary remark can also be made on the observation of an extra frequency stably clustered around 1 Hz in Fig. 5(b). It has been noticed that certain modal frequencies of bridge deck can be identified from the cable vibration measurements (Wu *et al.* 2016a, Chen *et al.* 2008). This frequency actually corresponds to a dominant deck mode which can be confirmed in the following discussions for deck measurements of the same bridge and is perceptible in Fig. 5(b) because the first mode of Cable R17 in the neighborhood is greatly reduced. A more convincing verification for the criterion of Eq. (5) may be further presented by similarly reducing the contributions from all the odd modes in each cable measurement. In this case, the least common multiple for the periods of the remaining even modes becomes $T_2 \approx 0.5T_1$, the period of the second cable mode. Based on the change of quasi-period for such a modified signal, it can be forecasted that the critical threshold of time lag parameter would turn into $i_c = 200/(2 \times 0.9) \approx 110$ for Cable R33 and $i_c = 200/(2 \times 1.63) \approx 60$ for Cable R17, respectively. As exhibited in Fig. 6, the alternative stabilization diagrams corresponding to a suppression of all the odd modes undoubtedly verifies this drastic change predicted by Eq. (5).
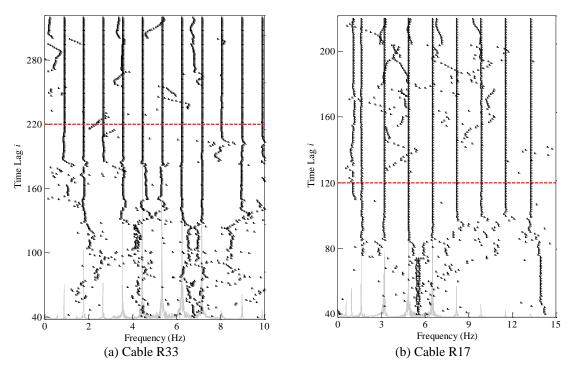
(a) Cable R33　　　　　　　　　　　　(b) Cable R17

Fig. 4 Alternative stabilization diagrams for single measurements of Cables R33 and R17
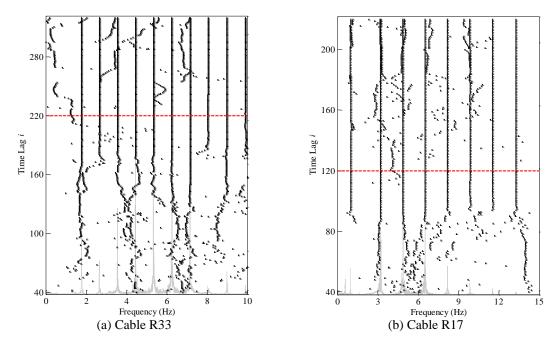

(a) Cable R33　　　　　　　　　　　　(b) Cable R17

Fig. 5 Alternative stabilization diagrams for single measurements of Cables R33 and R17 by suppressing the first mode

4.1.2 Deck measurements of Chi-Lu Bridge

The SSI analysis is then conducted with the single deck measurement D2 of Chi-Lu Bridge. Since there are 4 clear peaks (0.60 Hz, 0.98 Hz, 1.85 Hz, and 3.15 Hz) recognizable in the interested frequency range from 0 to 5 Hz of its FAS as shown in the background of Fig. 7(a), the system order is chosen as $n = 10$ and the time lag parameter is increased from $i_{\min} = i_0 = 20$ to $i_{\max} = 440$ in this case. In addition, the critical threshold can be obtained by $i_c = 200/0.6 \approx 330$ with the fundamental frequency $f_1 \approx 0.6\,\mathrm{Hz}$. Based on the corresponding stabilization diagram illustrated in Fig. 7(a), it is of no doubt that all the deck frequencies can be steadily identified when the criterion of $i \geq i_c = 330$ is approached. Similar to the artificial manipulation for cable measurements, the contribution of the first mode (0.6 Hz) for the single deck measurement D2 is further reduced in an interval of 1/3 Hz symmetrically bracketing that peak in the frequency domain. The alternative stabilization diagram corresponding to this modified signal is displayed in Fig. 7(b) where the lowest major mode is with a frequency of 0.98 Hz. Compared with Fig. 7(a), it is evidently observed from Fig. 7(b) that the critical threshold of time lag parameter in this case considerably drops to a lower level reliably estimated by $i_c = 200/0.98 \approx 210$ with the fundamental frequency of 0.98 Hz.
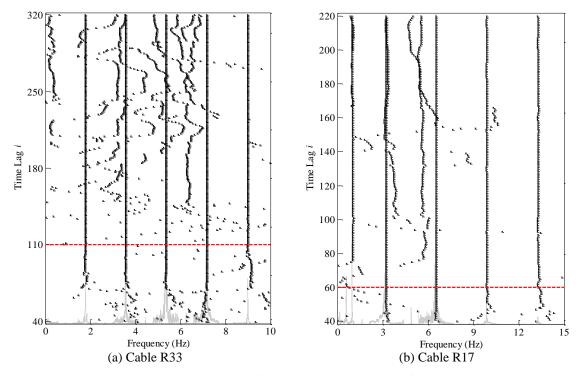

(a) Cable R33   (b) Cable R17

Fig. 6 Alternative stabilization diagrams for single measurements of Cables R33 and R17 by suppressing the odd modes
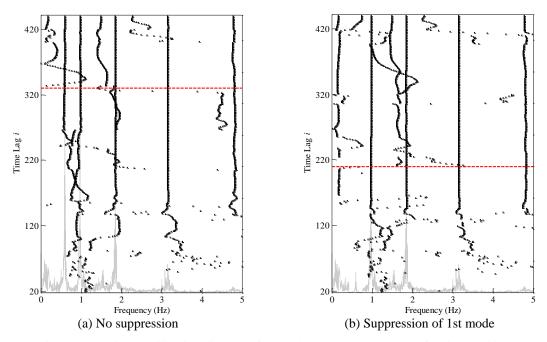
(a) No suppression	(b) Suppression of 1st mode

Fig. 7 Alternative stabilization diagrams for the deck measurement D2 of Chi-Lu Bridge

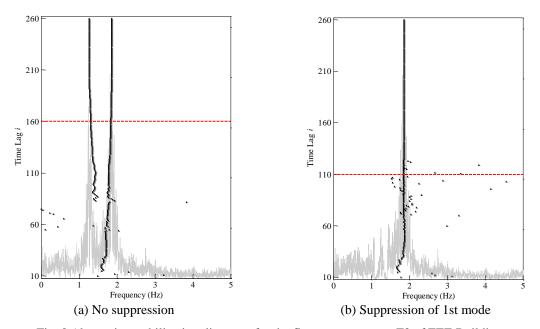|	
(a) No suppression	(b) Suppression of 1st mode

Fig. 8 Alternative stabilization diagrams for the floor measurement F3 of EEE Building

4.1.3 Floor measurement of EEE Building

The single floor measurement F3 of EEE Building is next considered for SSI analysis to provide the third type of structure examined in this study. Demonstrated in the background of Fig. 8(a), two major peaks (1.30 Hz and 1.86 Hz) can be found in the interested frequency range from 0 to 5 Hz of the FAS for this measurement and the system order is accordingly selected to be $n = 5$. Furthermore, the time lag parameter is increased from $i_{min} = i_0 = 10$ to $i_{max} = 260$ for constructing the alternative stabilization diagram shown in Fig. 8(a). With the fundamental frequency $f_1 \approx 1.25\,\mathrm{Hz}$, the critical threshold of i is decided by $i_c = 200/1.3 \approx 160$. It is again validated by Fig. 8(a) that the identified building frequencies become stable if the criterion of $i \geq i_c = 160$ is satisfied. The artificial manipulation to reduce the contribution of the first mode (1.3 Hz) is also applied in an interval of 1/3 Hz around this peak in the frequency domain and the corresponding stabilization diagram is depicted in Fig. 8(b). With a solely dominant frequency at 1.86 Hz in this case, it is clear that the critical threshold of time lag parameter is lowered to the level of $i_c = 200/1.83 \approx 110$ as forecast by Eq. (5). Based on the investigation in this subsection, the criterion of Eq. (5) is found to be applicable to single measurements for different types of structures.

4.2 Multiple measurements

For the simplicity of investigation, single measurements are first explored in the previous subsection. It is more often in typical engineering applications that multiple measurements are simultaneously taken to obtain convincing modal parameters including the mode shape vectors. Therefore, the SSI analysis with multiple measurements from the stay cable of Chi-Lu Bridge, the deck of Chi-Lu Bridge, and the floor of EEE Building is further probed in this subsection.
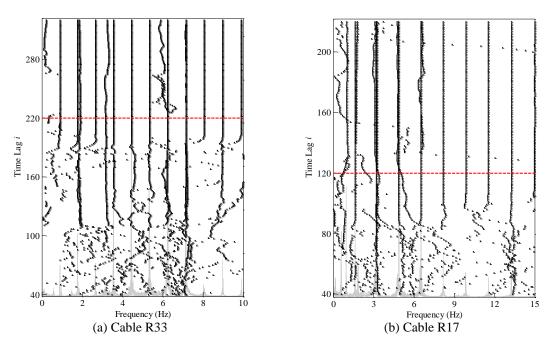

(a) Cable R33   (b) Cable R17

Fig. 9 Alternative stabilization diagram for multiple measurements of Cables R33 and R17

4.2.1 Cable measurements of Chi-Lu Bridge

As illustrated in Fig. 1, four sensors were installed on Cable R33 of Chi-Lu Bridge at different locations near the deck end to measure the ambient vibration signals. With the system order fixed at $n = 20$ and the time lag parameter increasing from $i_{min} = 40$ to $i_{max} = 320$, these four simultaneous measurements ($l = 4$) are adopted to perform the SSI analysis for constructing the alternative stabilization diagram portrayed in Fig. 9(a). Comparing Fig. 9(a) with the corresponding stabilization diagram in Fig. 4(a) for a single measurement, it is evident that the critical threshold for the time lag parameter is close to the same predicted value of $i_c = 220$ in both cases. Additionally, the alternative stabilization diagram for four simultaneous measurements taken on Cable 17 with the system order parameter set at $n = 20$ is also plotted in Fig. 9(b) from $i_{min} = 40$ to $i_{max} = 220$. Likewise, the critical threshold around $i_c = 120$ demonstrated in Fig. 9(b) for multiple measurements of Cable R17 is basically the same as that shown in Fig. 4(b) for a single measurement.

4.2.2 Deck measurements of Chi-Lu Bridge

As also displayed in Fig. 1, five velocimeters (D1 to D5) were distributed along the deck of Chi-Lu Bridge to conduct the ambient vibration measurements. With the same parameter selections ($n = 10$ and i from $i_{min} = 20$ to $i_{max} = 440$) as those for the case of single measurement in the SSI analysis, the alternative stabilization diagram corresponding to the five simultaneous measurements ($l = 5$) is shown in Fig. 10(a). Focusing on examining the four dominant deck frequencies demonstrated in Fig. 7(a), Fig. 10(a) discloses that the critical threshold for the time lag parameter is undoubtedly decreased from $i_c = 330$ in the case of single measurement to a much lower value at around 120 in the case of multiple measurements. Therefore, a thinner dashed line in red is adopted in Fig. 10(a) to indicate that $i_c = 330$ determined by Eq. (5) is definitely an overestimation in this case. To further inspect such an trend totally different from that for cable

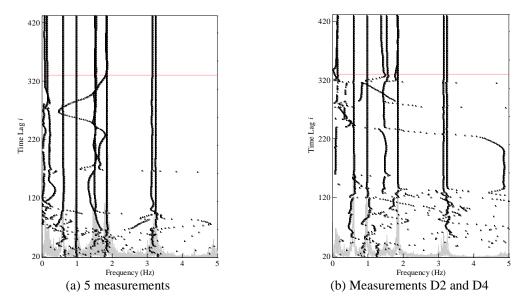(a) 5 measurements   (b) Measurements D2 and D4

Fig. 10 Alternative stabilization diagrams for multiple deck measurements of Chi-Lu Bridge

measurements, the alternative stabilization diagram corresponding to the use of two measurements D2 and D4 ($l = 2$) is presented in Fig. 10(b) as well. It is found that the critical threshold of the time lag parameter demonstrated in Fig. 10(b) for double measurements is close to 180. In other words, the critical threshold of i seems to decrease with the number of analyzed deck measurements. Other than the four clear frequencies identified in Fig. 7(a) for the single deck measurement D2, it is also noteworthy that one more stable frequency can be observed in Fig. 10(b) for the case with two deck measurements and two more steady frequencies are found in Fig. 10(a) for the case with five deck measurements. This phenomenon is not unusual in the practical applications of SSI analysis.

4.2.3 Floor measurements of EEE building

It is then interesting to check how the critical threshold of the time lag parameter would behave in the SSI analysis for the measurements from the other type of structure. As exhibited in Fig. 3, four sensors (F1 to F4) were installed on EEE Building to record the synchronized vibration signals of different floors. As in the case of single measurement, the same parameter selections with $n = 5$ and i from $i_{min} = 10$ to $i_{max} = 260$ are employed in the SSI analysis for multiple measurements. The alternative stabilization diagram corresponding to all the four measurements ($l = 4$) is plotted in Fig. 11(a) and the other associated with the use of two measurements F1 and F4 ($l = 2$) is depicted in Fig. 11(b). Comparison of Figs. 8(a), 11(a), and 11(b) clearly reveals that the critical threshold for the time lag parameter is almost the same with $i_c = 160$ in all the three cases. Accordingly, the situation for building measurements is similar to that for cable measurements and the critical threshold of i predicted by Eq. (5) is practically applicable to both cases no matter single or multiple measurements are analyzed. If multiple measurements of bridge deck are considered in the SSI analysis, however, Eq. (5) intends to make an overestimation. This tendency will be explored in the next section to seek for reasonable explanations.
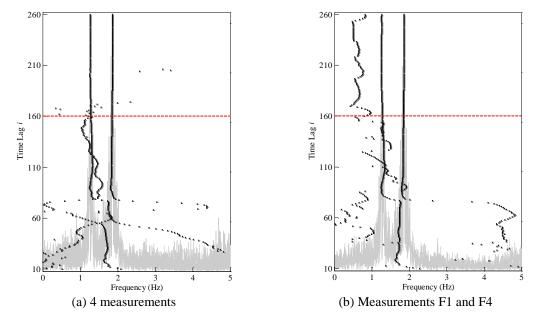

(a) 4 measurements   (b) Measurements F1 and F4

Fig. 11 Alternative stabilization diagrams for multiple floor measurements of EEE Building

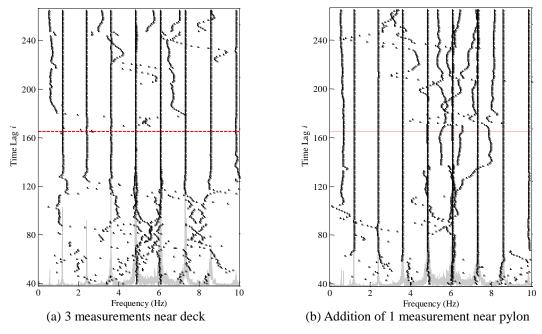(a) 3 measurements near deck

(b) Addition of 1 measurement near pylon

Fig. 12 Alternative stabilization diagrams for multiple measurements of Cable C16

5. Effect of independent excitations

As mentioned in Section 2, the identification of modal parameters based on the SSI analysis is supposed to be insensitive to the time lag parameter if the excitation is not far away from the white-noise assumption. For practical applications where narrowly banded excitations are usually encountered, a critical threshold for the time lag parameter to produce stable identification results is obtained in the form of Eq. (5) by considering the distribution of all the possible independent patterns associated with the covariance matrix in the Toeplitz matrix. Other than the cases of stay cables (Wu *et al*. 2014, Wu *et al*. 2016a), it has been demonstrated in the previous section that Eq. (5) is also valid for several applications with the measurements from bridge decks or buildings. To explain the exceptional case in which Eq. (5) obviously overestimate the critical threshold for the analysis with multiple measurements of the bridge deck, the key factor may also reside in the characteristics of excitations. For the three types of signals investigated in Section 4, their independent sources of excitation are not the same. The cable measurements of Chi-Lu Bridge are all taken near the deck end and there is only one major excitation source from the motion of bridge deck in this case. Similarly, the floor vibrations of EEE Building are principally induced by a single excitation source from the ground. On the other hand, the deck measurements of Chi-Lu Bridge are influenced by multiple excitations independently coming from the passing vehicles in the neighborhood of each sensor location. It is consequently suspected that numerous independent excitations in the case with multiple measurements of the bridge deck create an input more widely distributed in the frequency domain. Therefore, the critical threshold for the time lag would be significantly lowered in this case to approach the situation that the identified results are insensitive to *i* under the white noise excitation.

(a) 3 measurements near deck
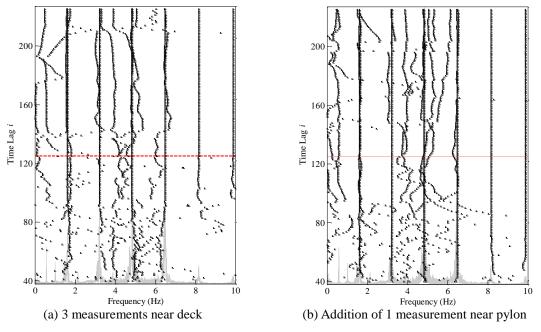

(b) Addition of 1 measurement near pylon

Fig. 13 Alternative stabilization diagrams for multiple measurements of Cable C13

To solidify the above conjecture, the ambient vibration measurements on Cables C16 and C13 of Shin-Dong Bridge would provide a perfect testimony. In addition to the installation of three velocimeters near the deck end of cable, the other velocimeter was mounted on a location close to the pylon end. Since the excitation for the pylon is considerably different from that for the deck, inclusion of the measurement near the pylon end in the SSI analysis is very likely to widen the contributed frequency range of excitation. For comparison, the alternative stabilization diagram associated with the three measurements ($l = 3$) near the deck end of Cable C16 is shown in Fig. 12(a) and the other corresponding to the addition of one more measurement close to its pylon end ($l = 4$) is illustrated in Fig. 12(b). With 8 clear peaks observed in the interested frequency range from 0 to 10 Hz of its FAS as shown in the background of Fig. 12, the system order is fixed at $n = 20$ and the time lag parameter is increased from $i_{min} = i_0 = 40$ to $i_{max} = 265$ in this case. Moreover, the critical threshold can be predicted by $i_c = 200/1.2 \approx 165$ considering that the fundamental frequency of this cable is $f_1 \approx 1.2\,\text{Hz}$. It is obvious that the critical threshold for the time lag parameter follows the estimated value of $i_c = 165$ pretty well in Fig. 12(a). This trend is similar to that for multiple cable measurements of Chi-Lu Bridge discussed in the previous section. Nevertheless, the corresponding threshold is substantially lowered to a value at approximately 80 in Fig. 12(b). Such a phenomenon due to the inclusion of one more measurement near the pylon end resembles the observations in Fig. 10 for multiple deck measurements of Chi-Lu Bridge. The same comparison is also made for the measurements on Cable C13 with the alternative stabilization diagrams displayed in Figs. 13(a) and 13(b) for the case of three measurements near the deck end ($l = 3$) and that adding one more measurement close to its pylon end ($l = 4$), respectively. For this analysis, the system order is chosen as $n = 20$ and the time lag parameter is increased from $i_{min} = 40$ to $i_{max} = 225$. With the fundamental frequency of $f_1 \approx 1.61\,\text{Hz}$ for Cable

C13, its critical threshold $i_c = 200/1.61 \approx 125$ can then be determined from Eq. (5). As expected, the critical threshold for the time lag parameter is noticeably decreased from around $i_c = 125$ in Fig. 13(a) to a much lower value at about 60 in Fig. 13(b). An emphasis should be made that the cases by considering single measurements or one measurement close to the deck end together with the measurement near the pylon end are also extensively examined in this study. It is found that the stabilization diagrams corresponding to the cases with a single measurement are all similar to Fig. 13(a). On the other hand, the cases with one measurement near the deck end and the other close to the pylon end consistently hold the stabilization diagrams like Fig. 13(b). With all the above powerful evidences, it is not difficult to deduce that the identified results from the SSI analysis for the signals caused by more independent excitations would reach stable values under a much lower threshold of the time lag parameter than that estimated by Eq. (5).

6. Conclusions

Based on the alternative stabilization diagram by varying the time lag parameter in the SSI analysis, this study systematically investigates the measurements from three different types of civil structures to extend the applicability of a recently noticed criterion to ensure stable identification results. Such a criterion demands the time lag parameter to be no less than a critical threshold determined by the ratio of the sampling rate to the fundamental frequency of the system and is firstly validated for its applications with single measurements from stay cables, bridge decks, and buildings. Regarding multiple measurements, it is found that the predicted threshold works well for the cases of stay cables and buildings, but makes an evident overestimation for the case of bridge decks. This discrepancy is further explained by the fact that the deck vibrations are induced by multiple excitations independently coming from the passing traffic. The cable vibration signals covering the sensor locations close to both the deck and pylon ends of Shin-Dong Bridge provide convincing evidences to testify this important discovery.

Overall, this work clarifies the appropriate selection of the time lag parameter in constructing the alternative stabilization diagram associated with the SSI analysis for several types of civil structures. Even in the cases employing the conventional stabilization diagram, it also offers an excellent basis to determine the designated value of time lag parameter. For a more convenient application in structural health monitoring, the work is under way to create a doubly folded stabilization diagram by combining the advantages of the conventional and alternative stabilization diagrams. It is also hoped that the applications can be generalized to more types of structures and more interesting investigations in the near future. For example, comparison of the stabilization diagrams for cable and deck measurements under different wind speeds would be instructive for more systematically studying the wind effects on the modal parameters of cable-stayed bridges.

Acknowledgments

References

Bakir, P.G. (2011), "Automation of the stabilization diagram for subspace based system identification", *Expert Syst. Appl.*, **38**(12), 14390-14397.

Cara, F.J., Carpio, J., Juan, J. and Alarcon, E. (2012), "An approach to operational modal analysis using the expectation maximization algorithm", *Mech. Syst. Signal Pr.*, **31**, 109-129.

Cara, F.J., Juan, J., Alarcon, E., Reynders, E. and De Roeck, G. (2013), "Modal contribution and state space order selection in operational modal analysis", *Mech. Syst. Signal Pr.*, **38**(2), 276-298.

Carden, E.P. and Brownjohn J.M. (2008), "Fuzzy clustering of stability diagrams for vibration-based structural health monitoring", *Comput.-Aided Civil Infrastruct. Eng.*, **23**(5), 360-372.

Chen, C.C., Wu, W.H., Huang, C.H. and Lai, G. (2013), "Determination of stay cable force based on effective vibration length accurately estimated from multiple measurements" *Smart Struct. Syst.*, **11**(4), 411-433.

Chen, C.C., Wu, W.H., Leu, M.R. and Lai, G. (2016), "Tension determination of stay cable or external tendon with complicated constraints", *Measurement*, **86**, 182-195.

Chen, C.C., Wu, W.H. and Liau, J.A. (2008), "Modal frequency identification for cable and girder using ambient cable vibration signals" *J. Chin. Inst. Civ. Hydraul Eng.*, **20**(4), 509-521.

Deraemaeker, A., Reynders, E., De Roeck, G. and Kullaa, J. (2008), "Vibration-based structural health monitoring using output-only measurements under changing environment", *Mech. Syst. Signal Pr.*, **22**(1), 34-56.

Kompalka, A.S., Reese, S. and Bruhns, O.T. (2007), "Experimental investigation of damage evolution by data-driven stochastic subspace identification and iterative finite element model updating", *Arch. Appl. Mech.*, **77**(8), 559-573.

Loh, C.H., Lu. Y.C. and Ni, Y.Q. (2012), "SSA-based stochastic subspace identification of structures from output-only vibration measurements", *Smart Struct. Syst.*, **10**(4-5), 331-351.

Magalhaes, F., Cunha, A. and Caetano, E. (2009), "Online automatic identification of the modal parameters of a long span arch bridge", *Mech. Syst. Signal Pr.*, **23**, 316-329.

Magalhaes, F., Cunha, A., Caetano, E. and Brincker, R. (2010), "Damping estimation using free decays and ambient vibration tests", *Mech. Syst. Signal Pr.*, **24**(5), 1274-1290.

Mevel, L., Baseville, M. and Goursat, M. (2003), "Stochastic subspace-based structural identification and damage detection-application to the Z24 Bridge benchmark", *Mech. Syst. Signal Pr.*, **17**(1), 143-151.

Peeters, B. (2000), "System identification and damage detection in civil engineering", Ph.D. Dissertation, Katholieke Universiteit Leuven, Leuven.

Reynders, E. and De Roeck, G. (2008), "Reference-based combined deterministic-stochastic subspace identification for experimental and operational modal analysis", *Mech. Syst. Signal Pr.*, **22**(3), 617-637.

Reynders, E., Houbrects, J. and De Roeck, G. (2012), "Fully automated (operational) modal analysis", *Mech. Syst. Signal Pr.*, **29**, 228-250.

Reynders, E., Pintelon, R. and De Roeck, G. (2008), "Uncertainty bounds on modal parameters obtained from stochastic subspace identification", *Mech. Syst. Signal Pr.*, **22**(4), 948-969.

Sampaio, R. and Chan, T.H.T. (2015), "Modal parameters identification of heavy-haul railway RC bridges – experience acquired", *Struct. Monit. Maint.*, **2**(1), 1-18.

Scionti, M. and Lanslots, J.P. (2005), "Stabilisation diagrams: pole identification using fuzzy clustering techniques", *Adv. Eng. Softw.*, **36**(11), 768-779.

Ubertini, F., Gentile, C. and Materazzi, A.L. (2013), "Automated modal identification in operational conditions and its application to bridges", *Eng. Struct.*, **46**, 264-278.

Van Overschee, P. and De Moor, B. (1991), "Subspace algorithm for the stochastic identification problem", *Proceedings of the 30th IEEE Conference on Decision and Control*, Brighton, England, December.

Van Overschee, P. and De Moor, B. (1993), "Subspace algorithms for the stochastic identification problem", *Automatica*, **29**(3), 649-660.

Van Overschee, P. and De Moor, B. (1996), *Subspace Identification for Linear Systems:*

Theory-Implementation-Applications, Kluwer Academic Publishers, Dordecht, Netherlands.

Wu, W.H., Chen, C.C., Wang, S.W. and Lai, G. (2014), "Modal parameter determination of stay cable with an improved algorithm based on stochastic subspace identification", *Proceedings of the 7th European Workshop on Structural Health Monitoring*, Nantes, France, July.

Wu, W.H., Wang, S.W., Chen, C.C. and Lai, G. (2016a), "Application of stochastic subspace identification for stay cables with an alternative stabilization diagram and hierarchical sifting process", *Struct. Control Health Monit.*, **23**(9), 1194-1213.

Wu, W.H., Wang, S.W., Chen, C.C. and Lai, G. (2016b), "Mode identifiability of a cable-stayed bridge under different excitation conditions assessed with an improved algorithm based on stochastic subspace identification", *Smart Struct. Syst.*, **17**(3), 363-389.

Yan, A.M. and Golinval, J.C. (2006), "Null subspace-based damage detection of structures using vibration measurements", *Mech. Syst. Signal Pr.*, **20**(3), 611-626.

SN